THE JOURNAL OF PHYSICAL CHEMISTRY C

pubs.acs.org/JPCC Article

Mn−Cu Transmetalation as a Strategy for the Assembly of Decoupled Metal−Organic Networks on Sn/Cu(001) Surface Alloys

P. Machaín, J. D. Fuhr, S. Schneider, S. Carlotto, M. Casarin, A. Cossaro, A. Verdini, L. Floreano, M. Lingenfelder, J. E. Gayone, and H. Ascolani*

Cite This: https://dx.doi.org/10.1021/acs.jpcc.0c03395 Read Online

ACCESS | Metrics & More | Article Recommendations | Supporting Information

ABSTRACT: Surface alloying of Cu(001) by Sn deposition is a finely controllable method of tuning the degree of copper reactivity in order to drive the on-surface assembly and synthesis of metal−organic coordination networks. In this work we show that the $(3\sqrt{2} \times \sqrt{2})R45°$ reconstruction of the Sn/Cu(001) surface alloy acts as a weakly interacting substrate ideal for the assembly of rectangular metal−organic networks based on transition metals. As a demonstration, we have grown a two-dimensional coordination network formed by manganese and TCNQ (7,7,8,8-tetracyanoquinodimethane) with 1:1 stoichiometry. In contrast with the same structure grown on Au(111), the use of the Sn/Cu(001) substrate enables a commensurate structure with larger and more regular ordered domains. We show that the formation of a Cu−TCNQ coordination network and subsequent Mn−Cu transmetalation reactions are the key steps of the growth mechanism. Moreover, ab initio density-functional calculations indicate that the system studied in the present work is a unique example of a metal−organic coordination network weakly interacting with the substrate.

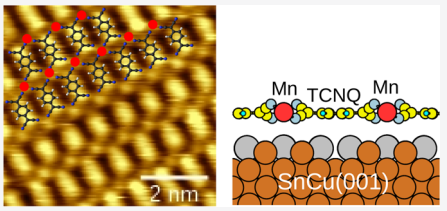

INTRODUCTION

The engineering of two-dimensional (2D) metal−organic networks (MOCNs) based on coordination bonds is motivated by the attractive magnetic and catalytic properties of these surface-confined materials.[1−4] The synthesis strategy consists of coevaporating the basic building blocks (metal atoms and molecules) on crystalline surfaces under fine control of the preparation parameters. The properties of the MOCNs depend on the chosen metal centers and ligands and also on their interactions with the underlying surface.[5] Thus, tuning the interactions of the chosen building blocks with the substrate is a relevant tool for MOCN engineering. A considerable limitation of this strategy found in the synthesis of rectangular MOCNs arises from the lack of weakly interacting metal substrates with rectangular symmetry. In this article we show that the surface alloy Sn/Cu(001) meets the requirements to satisfy this need.

Prototypical examples of 2D MOCNs are those based on transition metals (TMs) and TCNQ molecules (7,7,8,8-tetracyanoquinodimethane). Among the TMs, the cases of Mn and Ni have been widely and thoroughly studied both experimentally and theoretically.[6−13] On Au(111), both metal ions combined with TCNQ molecules to form rectangular networks with 1:1 stoichiometry and superexchange-mediated magnetic order.[8−11] Recent experiments show that the Ni−TCNQ overlayer is ferromagnetic at low temperatures without any magnetic anisotropy, while the Mn−TCNQ one presents antiferromagnetism with a weak in-plane anisotropy.[10] In the case of Ni−TCNQ, the absence of magnetic anisotropy had to be ascribed to a substrate effect, which reduces the anisotropy due to a combination of electronic charge transfer and change of Ni−N coordination. In contrast, the magnetic behavior of Mn−TCNQ could be fully described by a free-standing MOCN model, discarding the substrate interaction.

However, the substrate is never absolutely inert and its surface properties, such as symmetry, chemical reactivity, electronic properties, etc., affect the properties of the adsorbed MOCN. Indeed, the above-mentioned rectangular TM−TCNQ MOCNs assembled on Au(111) grows only in small domains on an incommensurate structure on the hexagonal surface. This fact is relevant to the development of future applications, since the impossibility of growing large ordered domains prevents the generalization of the approach. Clearly, a weakly interacting substrate with rectangular symmetry would be more suitable for rectangular MOCNs.

A pioneering study of the Mn−TCNQ assembly on the bare Cu(001) surface, revealed that the corresponding MOCN is strongly affected by the substrate interaction: half of the nitrile terminations are chemically bound to the Cu substrate, thus yielding an MOCN with a 1:2 Mn:TCNQ stoichiometry ratio, where adjacent tetracoordinated Mn centers are expected to yield weak magnetic coupling.[6] The assembly of Mn− and Ni−TCNQ$_x$ coordination structures on Ag(001) has also been

Received: April 16, 2020
Revised: August 10, 2020
Published: August 11, 2020

investigated, finding an intermediate behavior in between those observed for the same building blocks on Cu(001) and on Au(111).[7]

The interaction of the Cu(001) surface with adsorbed organic molecules can be strongly reduced by Sn alloying. In fact, the $(3\sqrt{2} \times \sqrt{2})R45°$ reconstruction of the Sn/Cu(001) interface (from now on abbreviated as $3\sqrt{2}$), consisting of 0.5 monolayer (ML) of Sn atoms embedded in the top surface layer of the Cu(001) crystal,[14,15] has already proven to be a robust substrate for self-assembled supramolecular structures.[16−19] In particular, we have shown in previous work that TCNQ molecules deposited on the $3\sqrt{2}$-Sn/Cu(001) substrate present a rich phase diagram where TCNQ forms different MOCNs with native Cu adatoms.[19]

A possible route to the formation of novel metal−organic structures on surfaces is by means of transmetalation reactions.[20−24] Very recently, Hötger et al. reported an interesting study of the Fe → Co transmetalation reaction taking place in Fe-porphyrins adsorbed on Au(111), where the reaction paths were theoretically analyzed with great detail.[25] This study showed that a direct "hit" mechanism is highly favorable due the fact that the exchange reaction is highly exothermic and the involved energy barriers are low.

Here, we show that a rectangular Mn−TCNQ coordination network can be grown on the $3\sqrt{2}$-Sn/Cu(001) substrate using a Cu → Mn transmetalation reaction, i.e., the replacement of the Cu cations of the initial Cu−TCNQ networks by deposited Mn atoms. Interestingly, the Mn−TCNQ network obtained on the $3\sqrt{2}$-Sn/Cu(001) substrate presents a rectangular structure very similar to what is formed on Au(111)[8] but commensurated and forming large ordered domains. Our ab initio density-functional calculations indicate that the studied system is a unique example of MOCNs that show very little interaction with the substrate.

EXPERIMENTAL AND COMPUTATIONAL METHODS

The experiments reported in the present work have been performed in two different laboratories. The experiments of scanning tunneling microscopy (STM) were performed at the Centro Atómico Bariloche, Argentina, while the X-ray photoemission spectroscopy (XPS) experiments were carried out at the ALOISA beamline[26,27] of the ELETTRA synchrotron in Trieste, Italy.

The STM chamber is equipped with a low-energy electron diffraction (LEED) optics, a homemade sputtering gun, and evaporators. The Cu(001) substrate (Mateck, orientation accuracy ±0.1°) was prepared by repeated cycles of Ar^+ bombardment at 1.5 keV and followed by an annealing process held at 500 °C. Half monolayer of tin was evaporated onto the clean Cu(001) surface kept at room temperature (RT) to form the $3\sqrt{2}$-Sn/Cu(001) at a rate of 0.1 ML every 2.5 min. The formation of the $3\sqrt{2}$ structure was checked by means of LEED. The procedure used to prepare all the Mn based MOCN on the $3\sqrt{2}$-Sn/Cu(001) substrates shown in this work is the following. First, the TCNQ molecules were evaporated on the $3\sqrt{2}$-Sn/Cu(001) substrate kept at 150 °C, followed by a cooling-down step to RT, enabling the formation of ordered Cu−TCNQ networks on the $3\sqrt{2}$-Sn/Cu(001) substrate. Subsequently, Mn atoms were deposited on the prepared Cu−TCNQ/$3\sqrt{2}$-Sn/Cu(001) surface kept at a fixed temperature. The TCNQ molecules (Sigma-Aldrich, 98% purity) were evaporated from the homemade boron nitride (BN) Knudsen cells. The molecular evaporation rate was of approximately 1/12 ML every 6 min, where 1 ML of molecules is defined as the coverage corresponding to 1 molecule or atom per Cu(001) surface unit cell. In the STM chamber, manganese was evaporated from a homemade boron nitride (BN) Knudsen cell with an evaporation rate of ∼0.05 ML/min. All the STM images reported in this work were taken at RT using W tips.

The XPS spectra were measured in normal emission by means of an hemispherical electron analyzer (angular acceptance of 2°). For details of the preparation procedure at the ALOISA beamline, see section SI-1 of the Supporting Information. We measured the Mn 2p, Sn 3d, N 1s, and Cu 3p photoemission spectra with a photon energy of 800 eV and an overall energy resolution of 300 meV. Additionally, with a photon energy of 515 eV (overall resolution of 230 meV), we measured the N 1s, C 1s, Cu 3p, Sn 4d, and valence-band photoemission spectra. The binding energy of each spectrum is calibrated to the position of the Cu $3p_{3/2}$ peak.

We performed density functional theory (DFT) calculations using the Quantum ESPRESSO package,[28] a plane-wave implementation with pseudopotentials. In order to take into account molecule−surface van der Waals interactions, we used the vdW-DF2-B86R functional of Hamada,[29] which is a revised second version of the vdW-DF.[30] For the Mn atoms, we include an on-site Hubbard-like interaction in the simplified version of Cococcioni et al.,[31] with $U = 4.0$ eV. We used a wave function/charge cutoff of 55/440 Ry, and Brillouin integrations were done using a grid equivalent to 12 × 12 × 1 k-points for the Cu(001) surface unit cell. With these parameters, we obtained an optimized lattice parameter of 3.60 Å, which we used in the rest of the calculations. For the surface calculations, we have used the slab method with five Cu layers and the Sn alloy in the topmost layer. In all the calculations, we fixed the two lower layers while all other atoms are allowed to relax. For the calculation of transition energy barriers, we use the nudged elastic band (NEB)[32] method to obtain the minimum energy path (MEP).

RESULTS AND DISCUSSION

When TCNQ molecules are deposited on the $3\sqrt{2}$-Sn/Cu(001) substrate kept at 150 °C, followed by a cooling down step to RT, two coexisting coordination structures based on native Cu adatoms are observed forming large ribbon-type domains: the γ and β phases, where native Cu adatoms are bond to three and two nitrile groups, respectively (see Figure 1).[19] While the β-phase with a Cu:TCNQ ratio of 2:1 and a molecular coverage of 1/14 ML dominates at low coverages, the γ-phase with a Cu:TCNQ ratio of 1:1 and a molecular coverage of 1/12 ML dominates at coverages close to a saturated monolayer. A distinctive characteristic of the γ and β phases is the presence of TCNQ molecules azimuthally rotated with respect to the [100] crystallographic direction (see Figure 1). Regarding the range of thermal stability of the mixed Cu−TCNQ overlayer formed before Mn deposition, a conservative estimation of the maximum temperature at which its atomic structure does not change is ∼120 °C.[33] Additionally and only when the TCNQ molecules are deposited on the $3\sqrt{2}$-Sn/Cu(001) substrate kept at ∼RT, a third metal−organic phase with native Cu adatoms (α-phase) is observed (see Figure 1).

https://dx.doi.org/10.1021/acs.jpcc.0c03395
J. Phys. Chem. C XXXX, XXX, XXX−XXX

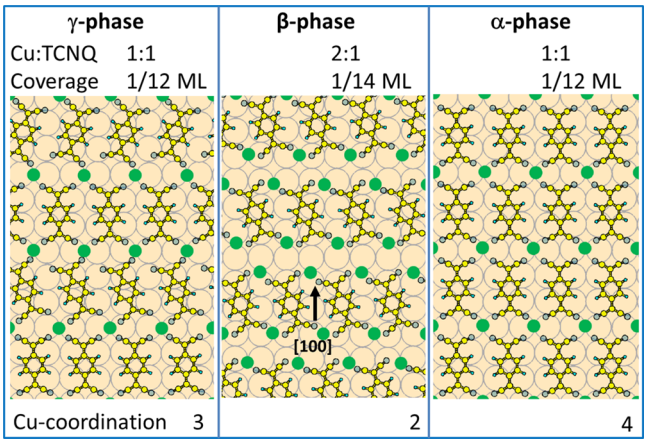

Figure 1. γ, β, and α Cu−TCNQ coordination structures formed when TCNQ molecules are deposited on the $3\sqrt{2}$-Sn/Cu(001) substrate. The corresponding coordination numbers of the Cu cations, Cu:TCNQ ratios, and molecular coverages of the three phases are indicated. The green circles represent Cu adatoms. Only the Sn atoms of the $3\sqrt{2}$-Sn/Cu(001) substrate are shown.

In this case, each Cu cation is coordinated to four molecules with a Cu:TCNQ ratio of 1:1, forming a rectangular unit cell.[19]

The $(3\sqrt{2} \times 2\sqrt{2})R45°$ Mn−TCNQ Network. Figure 2a shows an STM image of the surface resulting from depositing Mn on the Cu−TCNQ/$3\sqrt{2}$-Sn/Cu(001) interface kept at 80 °C. As discussed above, at this temperature, the Cu−TCNQ overlayer (formed by the β and γ phases) is structurally stable. The surface presents extended ribbon-shaped domains, similar to the Cu−TCNQ ones, where the TCNQ molecules (elongated protrusions) are arranged in parallel configurations. In the surface areas free of molecules, the observed parallel lines correspond to the $3\sqrt{2}$ reconstruction and are oriented along the [100] and [010] crystallographic directions.[15] A close inspection of the ribbons indicates that they contain relatively large areas where the molecules form a highly ordered rectangular pattern. In addition, there are other regions, where the molecules appear to be azimuthally rotated with respect to the axis of the ribbon. The fraction of rectangular structure increases with the dose of the manganese, and therefore, this phase is related to the presence of Mn atoms on the surface. We thus attribute the azimuthally rotated molecules observed in the ribbons of Figure 2a to residues of Cu−TCNQ networks.

Figure 2b and Figure 2c show high-resolution images of regions where the molecules follow a rectangular arrangement. The empty-state image (Figure 2b) shows a highly regular pattern of prominent rounded protrusions located at the "hollow" sites formed by four adjacent molecules. With opposite bias polarity (Figure 2c) the molecules present an internal structure that resemble the shape of the TCNQ lowest unoccupied molecular orbital (LUMO), while the protrusions become less intense and diffuse but are nonetheless visible. Since the Cu-adatoms in the Cu−TCNQ structures are unlikely detected by the STM,[19] and the rectangular α-phase is not present before Mn deposition, we may conclude that the observed rounded protrusions cannot be coordinated Cu adatoms and instead they identify the presence of Mn coordination centers.

This rectangular structure has a unit cell containing one molecule, with its long axis parallel to the long side of the unit

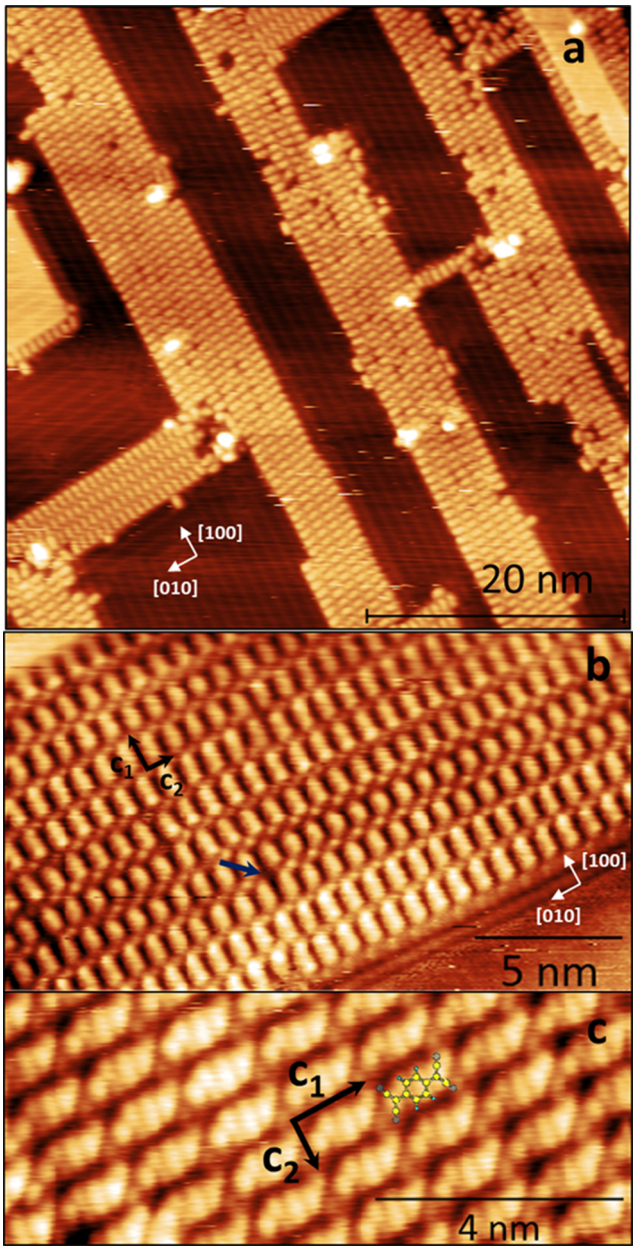

Figure 2. STM images of the metal−organic overlayer formed after deposition of Mn on a Cu−TCNQ/$3\sqrt{2}$-Sn/Cu(001) interface kept at 80 °C. (a) Empty-state image (2 V/150 pA). (b) Empty-state image (1.5 V/500 pA). The blue arrow indicates a site where the corresponding Mn atom is missing. The unit cell vectors c_1 and c_2 are indicated. (c) Filled-state image (−2 V/600 pA).

cell, and one small rounded protrusion. The modules of the vectors c_1 and c_2 of the unit cell are, as determined from STM images, (11.1 ± 0.5) Å and (7.3 ± 0.5) Å, respectively, whereas the subtended angle is 91 ± 2°. The size and orientation of the measured unit cell are consistent with a $(3\sqrt{2} \times 2\sqrt{2})R45°$ periodicity (10.83 Å × 7.22 Å), which suggests that the obtained rectangular structure could be commensurate with the $3\sqrt{2}$ reconstruction. This observation is strongly supported by the measured STM images and LEED patterns. As seen in Figure 2a, the orientation of the ribbons follows that of the stripes of the $3\sqrt{2}$ reconstruction, which implies a correlation between the overlayer structure and the reconstruction. See section SI-2 of the Supporting Information for details. In

https://dx.doi.org/10.1021/acs.jpcc.0c03395
J. Phys. Chem. C XXXX, XXX, XXX−XXX

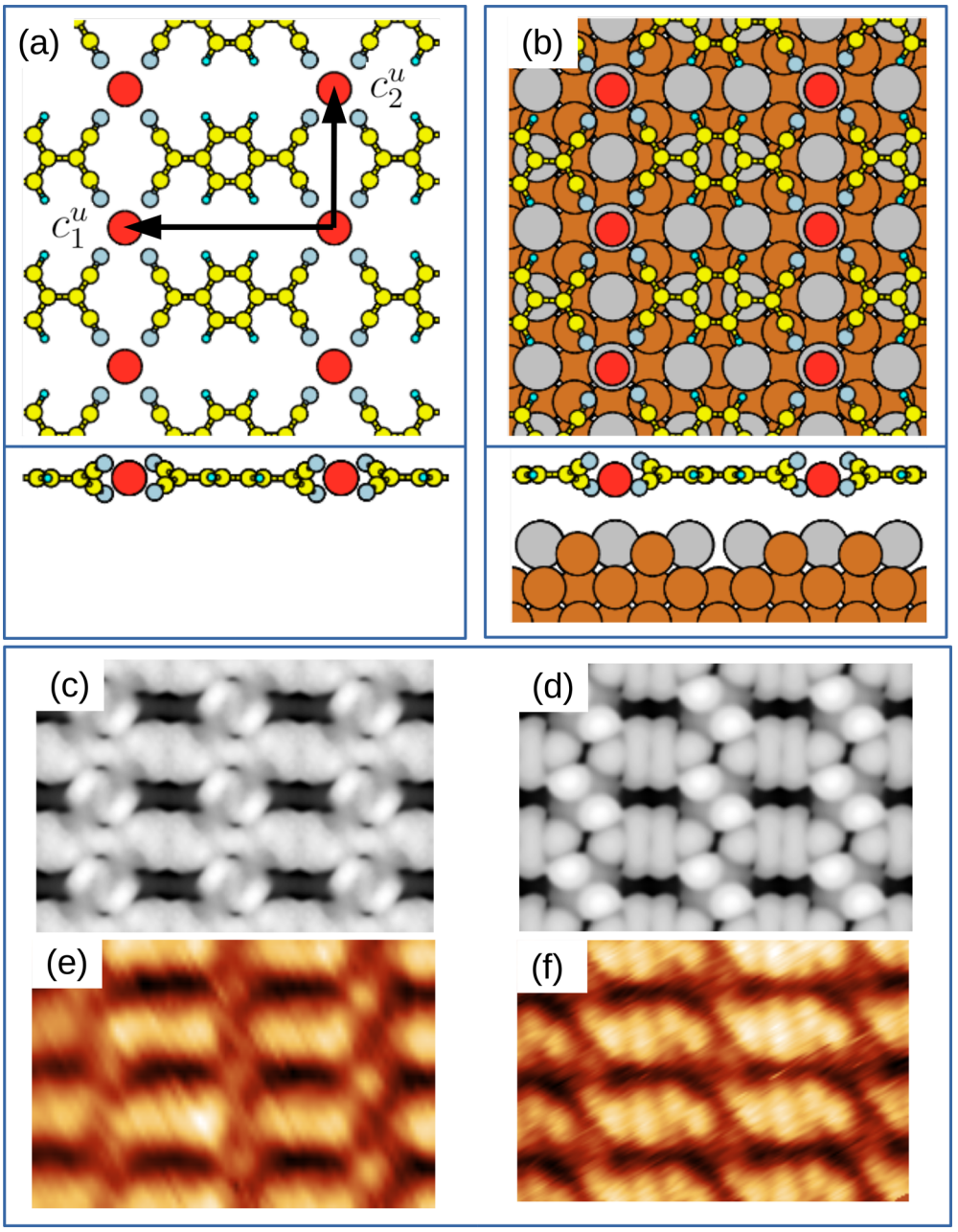

Figure 3. (a, b) Top and side views of the lowest-energy atomic configurations for a rectangular Mn−TCNQ monolayer: (a) unsupported and (b) adsorbed on the Sn−Cu(001) surface alloy with a $(3\sqrt{2} \times 2\sqrt{2})R45°$ unit cell. (c, d) Simulated STM images for the lowest-energy rectangular Mn−TCNQ monolayer adsorbed on the Sn−Cu(001) surface alloy: (c) positive bias (+2 V); (d) negative bias (−2 V). (e, f) Experimental empty- and filled-state STM images, respectively. These images were excerpted from those shown in Figure 2b and Figure 2c.

addition, the measured LEED patterns show fractional-order spots compatible with a $(3\sqrt{2} \times 2\sqrt{2})R45°$ superstructure. See section SI-3 of the Supporting Information for details. We therefore conclude that the obtained rectangular structure is commensurate with the underlying surface reconstruction. As a consequence, the corresponding molecular coverage is 1/12 ML.

It is well established in the literature that the TCNQ molecules form rectangular structures similar to the one obtained in the present work with a variety of metals, including Mn,[8] Cu,[19] and Sn.[34] In this particular case, the Sn-mediated coordination can be discarded since the Cu−nitrile coordination bonds are dominant over the Sn−nitrile bonds.[19,34] The rectangular Mn−TCNQ network, with a Mn:TCNQ ratio of 1:1 and each Mn atom coordinating four TCNQ molecules by their nitrile groups, seems to be the most reasonable candidate for the obtained structure. Although geometrically similar to the RT α phase of Cu−TCNQ, the structure of the Mn−TCNQ unit cell is predicted to be significantly different in terms of adsorption sites and molecular conformation, as will be shown hereafter.

A DFT relaxation of an unsupported rectangular Mn−TCNQ network results in the stable structure shown in Figure 3a, with unit cells vectors c_1^u = 11.31 Å and c_2^u = 7.05 Å and a subtended angle of 90.8°. This unit cell is very close to the one obtained from the rectangular network experimentally synthesized in this work (Figure 2). Additionally, this

https://dx.doi.org/10.1021/acs.jpcc.0c03395
J. Phys. Chem. C XXXX, XXX, XXX−XXX

unsupported Mn−TCNQ network is also very similar to the theoretical structure reported by Ma et al.[12] However, in the latter, only planar configurations were considered, while in our DFT relaxations we obtained a twisting of the $C(CN)_2$ groups of the TCNQ molecules resulting in a nonplanar structure.

We performed DFT calculations of the Mn−TCNQ monolayer on the $3\sqrt{2}$-Sn/Cu(001) substrate, considering a $(3\sqrt{2} \times 2\sqrt{2})R45°$ superstructure. The specific registry of the overlayer with respect to the $3\sqrt{2}$ reconstruction was derived from the analysis of the STM images (see section SI-2 of the Supporting Information). We started from several initial configurations with the Mn atoms placed at both higher and lower levels with respect to the plane defined by the TCNQ rings. We evaluated two different adsorption sites for the Mn cations: (i) hollow sites formed by two Sn atoms and two Cu atoms and (ii) atop Sn atoms. The results show that the latter is the most stable configuration with an energy gain of 60 meV (see section SI-6 of the Supporting Information for more details). Figure 3b shows top and side views of the lowest-energy geometric configuration. The Mn−TCNQ layer is found to be very weakly coupled to the substrate: the calculation indicates that the Mn cations are located at 3.40 Å from the Sn layer and only 0.25 Å below the C-rings of the TCNQ molecules.

The Mn−TCNQ structure assembled on the $3\sqrt{2}$-Sn/Cu(001) substrate is essentially the same as that obtained with the same calculation framework for the free-standing rectangular Mn−TCNQ structure (Figure 3a). In particular, the N−Mn distances are very similar, 2.11 Å in the unsupported case compared to 2.08−2.11 Å when the substrate is present (for comparison, a N−Mn distance of 1.96 Å is calculated for an isolated Mn−phthalocyanine molecule).[35] In both cases the structures present a significant twisting of the CN groups, with two N atoms below and two above the plane of the Mn atoms.

We simulated the STM images, using the Tersoff−Hamann approximation,[36] for the lowest-energy atomic configuration obtained for the Mn−TCNQ monolayer adsorbed on the Sn/Cu(001) surface alloy. Figure 3c and Figure 3d show the resulting simulated images for positive (empty states) and negative (filled states) bias, respectively. For both bias polarities there are bright spots in the positions defined by the encounter of four molecules. For positive bias, these spots are much brighter than the molecular ones, and they are associated with the Mn atoms. For negative bias, the simulated image puts in evidence the dominating contribution from the specific N atoms that are displaced above the C-rings plane due to the aforementioned twisting of the CN groups, in agreement with experimental observations. Comparing the images of Figures 3e and 2f, we note that the calculated images reproduce qualitatively the experimental observations.

The Mn−TCNQ layer is then at the same time commensurate with a $(3\sqrt{2} \times 2\sqrt{2})R45°$ superstructure and weakly interacting with the substrate. This fact can be rationalized as follows. The difference in the calculated lattice parameters between the fully relaxed unsupported Mn−TCNQ network (Figure 3a) and the $(3\sqrt{2} \times 2\sqrt{2})R45°$ unit cell is only −1.7% (+4.9%) in the short (long) side. Consistently, the energy cost associated with this distortion is low (0.1 eV/unit cell). On the other hand, we estimate (see SI-6 of the Supporting Information for details) the corrugation of the adsorption energy surface to be of the same order ($\gtrsim$0.1 eV). The fact that the obtained Mn−TCNQ MOCN is commensurate implies that the subtle interplay between the elastic energy cost and the adsorption energy surface corrugation is dominated by the latter. A similar case of a weakly coupled and commensurate MOCN has recently been reported for potassium coadsorption of TCNQ on Ag(111).[24]

The formation of a Mn-coordinated MOCN implies the displacement, by the deposited Mn atoms, of the Cu cations from the previously prepared Cu−TCNQ networks. Hereafter we analyze, by means of DFT calculations, the possible final locations of the displaced Cu atoms. We shall show that the energy barriers related to the reincorporation of these Cu atoms into the substrate are low enough that these processes are effective at the preparation temperatures used in this work.

It is revelant to compare the obtained Mn−TCNQ MOCN with a similar network on the Au(111) surface reported by Faraggi et al.[8] To calculate theoretically the system, the authors considered a $\begin{pmatrix} 9 & 2 \\ 1 & 3 \end{pmatrix}$ superstructure with a unit cell with sides of 23.6 and 7.6 Å and a subtended angle of 88.68° and containing two TCNQ molecules and two Mn atoms. This is comparable to a double unit cell in the long direction of the Mn−TCNQ network reported here, which results in sides of 22.2 and 7.3 Å. The similarity in the synthesized Mn−TCNQ networks in the two substrates suggests that the formation energy of the metal−organic overlayer is high compared with the interaction energies of the building blocks with these surfaces. The influence of the substrate is not negligible in neither of the two cases, but it is worth stressing that our theoretical predictions indicate that it is considerably weaker in the case of the $3\sqrt{2}$-Sn/Cu(001) substrate. In fact, DFT calculations by Faraggi et al. predict a bending of the TCNQ molecules with a vertical distance, Δ_z, between the C-ring and the Mn atoms of 0.5 Å and a Mn−substrate distance of 2.8 Å. In the present case, we see a negligible bending (Figure 3b), together with a smaller Δ_z (0.25 Å) and a larger Mn−substrate distance of 3.40 Å.

A significant advantage of the $3\sqrt{2}$-Sn/Cu(001) substrate with respect to the Au(111) surface is to allow the formation of long ribbon-shaped domains. Faraggi et al. stressed the tendency of their system to form a conglomerate of amorphous and rather small domains instead of single large domains and attributed this limitation to the interaction of the overlayer with the Au(111) surface. As a reference, the largest Mn−TCNQ domain reported by these authors has ∼200 nm^2. In the present case, the growth mode of the Mn−TCNQ coordination structure is different: it forms long ordered ribbons oriented parallel to the stripes of the $3\sqrt{2}$ reconstruction (Figure 2a). The length of the ribbons is limited only by the size of the $3\sqrt{2}$ reconstruction domains, although it was observed that in some cases they overcome small crossed $3\sqrt{2}$ domains. See section SI-2 of the Supporting Information for large scale images. Therefore, the use of the $3\sqrt{2}$-Sn/Cu(001) surface alloy as substrate would constitute a remarkable improvement with respect to the Au(111) because it allows the growth of long ordered ribbons of a nearly ideal Mn−TCNQ networks.

Replacement of the Cu Cations and Assembly of the Mn−TCNQ Network. The fact that the shape of the Mn−TCNQ domains in Figure 2a is very similar to the original Cu−TCNQ domains before the Mn deposition indicates a replacement process of the Cu cations by Mn atoms. The STM

https://dx.doi.org/10.1021/acs.jpcc.0c03395
J. Phys. Chem. C XXXX, XXX, XXX−XXX

images in Figure 4 illustrate the case where an insufficient amount of Mn atoms was deposited on the Cu−TCNQ surface kept at RT. Small domains of the rectangular Mn−TCNQ structure are visible in the STM image, although it presents different types of defects, as indicated by the enlarged images shown in panels b, c, d, and e. In order to analyze these images, it is important to take into account that the presence of TCNQ molecules with unsaturated nitrile groups on the pristine $3\sqrt{2}$-Sn/Cu(001) substrate is highly unlikely, due to the high energy gain related to the formation of Cu−nitrile coordination bonds and to the abundance of native Cu adatoms.[19] We also recall that a characteristic feature of the Cu−TCNQ β phase (as seen by the STM) is the presence of dark straight lines between molecular rows. As a consequence, the apparent vacant sites and the dark straight segments observed in Figure 4 can be confidently assigned to residual Cu−TCNQ domains. Figure 4b shows the Mn−TCNQ arrangement but with some of the TCNQ molecules displaying a small in-plane rotation, like in the Cu−TCNQ γ phase. Similarly, Figure 4c shows the regular Mn−TCNQ MOCN structure, where some of the Mn atoms are missing. In these sites, the Cu cations are coordinated to four nitrile groups, as in the Cu−TCNQ α phase. Finally, Figure 4d and Figure 4e highlight cases where the molecules are locally oriented like in the Cu−TCNQ β and γ phases, respectively, also indicating that some molecules are still coordinating Cu cations. In summary, these images show that a gradual replacement process of the Cu cations by Mn atoms takes place, even at RT, resulting in a metal−organic overlayer with a mix of Cu and Mn cations.

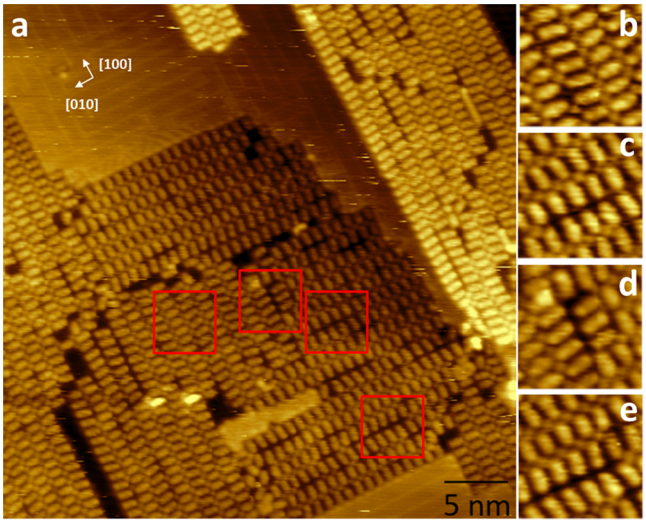

Figure 4. (a) STM image of a Mn/TCNQ/$3\sqrt{2}$-Sn/Cu(001) surface with an insufficient quantity of deposited Mn atoms: empty-state image (1.6 V/200 pA). The Mn atoms were deposited at RT on a previously prepared Cu−TCNQ/ $3\sqrt{2}$-Sn/Cu(001) interface. (b−d) Enlarged regions obtained from (a).

The transmetalation reaction taking place in the present case seems to present higher complexity than those observed in the cases of surface-supported metalloporphyrins. In the present case, the exchange of cations is accompanied by a slight molecular rearrangement. The coordination numbers of the Cu cations in the β and γ phases of the Cu−TCNQ networks are 2 and 3, respectively, whereas the Mn cations usually act with a coordination number of 4. These changes in the coordination order of the cation drive the molecular rearrangement. The fact that the structure of the γ phase is very close to that of the Mn−TCNQ network, both having the same molecular density, enables an easy transformation from one MOCN to the other one through the replacement of the Cu atoms by Mn ones. In contrast, when the replacement occurs on the Cu−TCNQ β phase, a different assembly process takes place due to the different molecular densities. In fact, the β phase is dominant at low coverage, thus facilitating the in plane displacement of TCNQ. In both cases, the molecular rearrangements involve only relatively small displacements and in-plane rotations, implying that the morphology of the β and γ phases of the Cu−TCNQ overlayer largely dictates that of the resulting Mn-based MOCN. In particular, the ribbon shape (Figure 2a) is essentially derived from the Cu−TCNQ networks.[19]

To address potential chemical changes that come along with the Cu cations replacement by Mn ones, we performed high-resolution XPS experiments focused on the Mn 2p, N 1s, and C 1s core levels. Figure 5 summarizes the results of a XPS experiment designed to investigate the activation barriers involved in the formation process of the Mn−TCNQ coordination structure. Specifically, spectra of the Mn 2p signal were measured as a function of the annealing temperature. As a reference, the spectrum in Figure 5a corresponds to a deposition of ∼1/8 ML of Mn atoms on the bare $3\sqrt{2}$-Sn/Cu(001) substrate. This spectrum is in agreement with the Mn 2p spectra reported for submonolayer amounts of Mn on transition metal substrates.[37−39] The broad $2p_{3/2}$ and $2p_{1/2}$ signals have their maxima at binding energies (BE) of about 639−640 eV and 650−651 eV, respectively. The

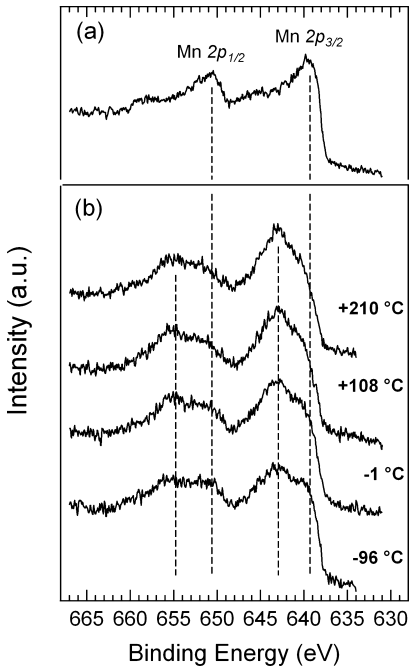

Figure 5. Mn 2p photoemission spectra measured with a photon energy of 800 eV: (a) spectrum obtained from ∼1/8 ML of Mn deposited at RT on the bare $3\sqrt{2}$-Sn/Cu(001) surface alloy; (b) ∼1/10 ML of Mn deposited on a Cu−TCNQ/$3\sqrt{2}$-Sn/Cu(001) interface kept at −100 °C. The four plotted spectra illustrate the evolution of the Mn 2p signal as a function of the sample temperature (indicated on the right).

https://dx.doi.org/10.1021/acs.jpcc.0c03395
J. Phys. Chem. C XXXX, XXX, XXX−XXX

observed complexity of the Mn 2p line shape, especially at the high BE tails, is attributed to the existence of multiple final states.

Figure 5b shows a selection of Mn 2p spectra measured on a Mn/Cu−TCNQ/3$\sqrt{2}$ interface prepared as follows. A Cu−TCNQ MOCN was prepared by molecular deposition at 150 °C, then the sample was cooled down to about −100 °C, and finally the Mn atoms were deposited on it. Subsequently, the evolution of the Mn 2p photoemission core-level signal was followed while increasing the sample temperature. Note that these spectra are remarkably different from the reference Mn/3$\sqrt{2}$ one (Figure 5a), which is representative of metallic manganese. In particular, the Mn $2p_{3/2}$ line corresponding to a temperature of −96 °C shows a peak at ∼643 eV and a shoulder at about 639−640 eV. The peak at ∼643 eV reflects the existence of a considerable quantity of strongly oxidized Mn atoms on the surface, which we attribute to the Mn atoms that have reacted with the TCNQ molecules through the formation of coordination bonds with the nitrile groups.

On the other hand, the shoulder on the low BE side is attributed to the presence of Mn atoms in metallic state on the surface, as it is aligned with the Mn $2p_{3/2}$ line representative of metallic Mn atoms (Figure 5a). Upon annealing, the Mn $2p_{3/2}$ line shape shows only minor changes up to 0 °C. Upon further annealing to +100 °C and beyond, a significant decrease of the metallic component and a corresponding increase of the reacted component take place.

Thus, the initial Mn 2p spectrum of Figure 5b indicates that at −96 °C a considerable fraction of the impinging Mn atoms have displaced Cu cations from the Cu−TCNQ networks. As the diffusion of the deposited Mn atoms on the surface is highly reduced at that temperature, the observed behavior strongly suggests that the Cu → Mn exchange processes is the result of direct "hit" events. This behavior is comparable with above-mentioned transmetalation reactions in surface-supported porphyrins.[25]

The evolution of the Mn 2p spectra with annealing temperature strongly suggests that further reaction of Mn atoms is inhibited up to 0 °C. At room temperature and above, the metallic Mn atoms can overcome the energy barriers for diffusion to the site of the coordinating Cu atoms and be incorporated in the TCNQ network. As can be observed in Figure 5b, a fraction of the original component of metallic Mn atoms is observed also after annealing to 210 °C. We can partly attribute this residual component to an excess of Mn deposited on the surface, as compared to the available reaction sites in the TCNQ network.

In fact, the amount of Mn atoms deposited in this experiment was estimated at ∼1/10 ML, whereas the molecular coverage of the TCNQ/3$\sqrt{2}$ interface was estimated at ∼1/15 ML. As a consequence, the Mn to TCNQ nominal ratio is 3:2, largely in excess of the 1:1 stoichiometry of the Mn−TCNQ MOCN. A quantitative analysis of the Mn 2p spectra is shown in section SI-4 of the Supporting Information.

To complement the study connected with Figure 5, we also analyzed two samples prepared by depositing Mn either at RT or at 150 °C, with a total amount of Mn atoms corresponding to a Mn:TCNQ ratio of 3:4 and 3:2, respectively. In both cases, the samples were annealed to 200 °C before XPS analysis. The analysis of the Mn 2p XPS (see Figure S6 of the Supporting Information for details) is equivalent to the one of Figure 5 (and Figure S5 of the Supporting Information), apart from different relative weights of the metallic vs coordinated Mn components. This observation confirms that the same Mn−TCNQ chemical configuration can be obtained at 150 °C.

The displaced Cu atoms could remain between the metallorganic layer and the surface, as was proposed in the case of transmetalation in porphyrins,[25] or they could be reincorporated into the substrate. We analyzed different configurations for the displaced Cu atoms by means of DFT calculations (see Figure S8 in section SI-6 of the Supporting Information for details of the considered structures). First, we started from a simple configuration equivalent to the α-phase of the Cu−TCNQ system with a Mn atom placed on top of the coordinated Cu atom. After relaxation, we found that the Mn replaced the Cu atom without any barrier, while the displaced Cu atom remained between the formed Mn−TCNQ MOCN and the substrate.

Subsequently, we analyzed the incorporation of the displaced Cu atom into the substrate. In this process, the key ingredient is the presence of intrinsic Cu vacancies of the 3$\sqrt{2}$-Sn/Cu(001) substrate, which can be filled by the displaced Cu atoms. We found that the system gains ∼0.30 eV when the displaced Cu atom occupies a vacancy site instead of remaining above the substrate. By means of a NEB calculation, we estimated that the energy barrier associated with the transition between the two specific configurations illustrated in Figure 6 is ∼0.17 eV. Hence, the reincorporation into the substrate of a displaced Cu atom has a low barrier when a nearby substrate Cu vacancy is available, and the process should be active at RT.

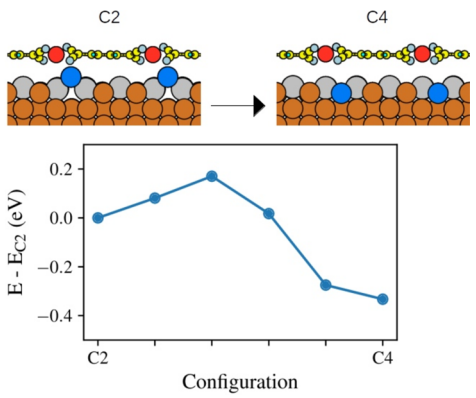

Figure 6. Energy profile along the minimum energy path when going from configuration C2 (top left), where the displaced Cu atom remains above the substrate, to configuration C4 (top right), where the dislaced Cu atom is filling a substrate Cu vacancy. See section SI-6 of the Supporting Information for more details about the C2 and C4 configurations.

The total-energy minimization calculations performed for the supported Mn−TCNQ structure with the displaced Cu atoms filling substrate vacancies show that the resulting MOCN is essentially the same as that shown in Figure 3, with a very small difference in regard to their MOCN−substrate interactions. Finally, the system gains an additional 0.40 eV by moving the displaced Cu atom from the outmost surface layer to the bulk, restoring the 3$\sqrt{2}$ reconstruction. The 3$\sqrt{2}$-Sn/Cu(001) surface presents a vacancy driven order−disorder phase transition at ∼90 °C.[40] Therefore, we

https://dx.doi.org/10.1021/acs.jpcc.0c03395
J. Phys. Chem. C XXXX, XXX, XXX−XXX

expect that during the preparation procedure applied in the case of the sample analyzed in Figure 2, where the Mn atoms were deposited with the surface kept at 80 °C, the in-plane mobility of the vacancies would be high enough to ensure that the displaced Cu atoms are incorporated in the substrate, obtaining at the end a Mn−TCNQ MOCN on top of the $3\sqrt{2}$ reconstruction.

CONCLUSION

The surface alloying of Cu(001) by Sn deposition is a finely adjustable method of tuning the degree of copper reactivity in order to drive the on-surface assembly and synthesis of metal−organic coordination networks. Deposition of TCNQ molecules on the $3\sqrt{2}$-Sn/Cu(001) substrate gives rise to MOCNs based on native Cu adatoms, but the strong interaction of TCNQ molecules with Cu atoms can be overcome by further reactions with transition metals to form 2D MOCNs of relevant magnetic interest.

In the present work, Mn atoms are incorporated in the TCNQ network by replacing the Cu cations via a transmetalation reaction, resulting in a weakly interacting Mn−TCNQ network with a configuration similar to that reported on the weakly interacting Au(111) substrate. Although the interaction of the Mn−TCNQ network with the surface is very weak in the cases of both substrates, the surface alloy shows clear advantages: (i) the obtained Mn−TCNQ network is commensurate with the substrate promoting larger ordered domains and allowing more precise theoretical simulations and (ii) the interaction of the Mn−TCNQ overlayer with the substrate is even weaker giving rise to a practically ideal 2D Mn−TCNQ overlayer.

The present result is relevant in the perspective of magnetic studies. Indeed, the replacement of the Cu cations embedded in coordination bonds with ligands based on nitrogen is not limited exclusively to manganese but it extends to most of TMs.[25,41] We thus expect that the $3\sqrt{2}$-Sn/Cu(001) substrate would enable the growth of a wide variety of 2D MOCNs based on TMs including the aforementioned ferromagnetic Ni−TCNQ network and also the Ni−TCNE (tetracyanoethylene) networks[42] that have recently been proposed as bipolar magnetic materials for spintronics.

ASSOCIATED CONTENT

Supporting Information

The Supporting Information is available free of charge at https://pubs.acs.org/doi/10.1021/acs.jpcc.0c03395.

Complementary information regarding (a) additional STM images, (b) experimental LEED patterns, (c) curve-fitting analysis of the Mn 2p XPS spectra obtained for different preparations, (d) the corresponding C 1s and N 1s XPS spectra, and (e) additional DFT calculations (PDF)

AUTHOR INFORMATION

Corresponding Author

H. Ascolani − *Centro Atómico Bariloche, CNEA y CONICET, R8402AGP Bariloche, Argentina;* orcid.org/0000-0002-9192-6604; Email: ascolani@cab.cnea.gov.ar

Authors

P. Machaín − *Centro Atómico Bariloche, CNEA y CONICET, R8402AGP Bariloche, Argentina*

J. D. Fuhr − *Centro Atómico Bariloche, CNEA y CONICET, R8402AGP Bariloche, Argentina; Instituto Balseiro, CNEA y Universidad Nacional de Cuyo, R8402AGP Bariloche, Argentina*

S. Schneider − *Centro Atómico Bariloche, CNEA y CONICET, R8402AGP Bariloche, Argentina*

S. Carlotto − *Department of Chemical Sciences, University of Padova, 35131 Padova, Italy;* orcid.org/0000-0003-0043-3538

M. Casarin − *Department of Chemical Sciences, University of Padova, 35131 Padova, Italy;* orcid.org/0000-0002-3347-8751

A. Cossaro − *CNR-IOM, Laboratorio TASC, I-34149 Trieste, Italy;* orcid.org/0000-0002-8429-1727

A. Verdini − *CNR-IOM, Laboratorio TASC, I-34149 Trieste, Italy;* orcid.org/0000-0001-8880-2080

L. Floreano − *CNR-IOM, Laboratorio TASC, I-34149 Trieste, Italy;* orcid.org/0000-0002-3654-3408

M. Lingenfelder − *Max Planck-EPFL Laboratory for Molecular Nanoscience, École Polytechnique Fédérale de Lausanne, 1015 Lausanne, Switzerland;* orcid.org/0000-0003-1362-8879

J. E. Gayone − *Centro Atómico Bariloche, CNEA y CONICET, R8402AGP Bariloche, Argentina; Instituto Balseiro, CNEA y Universidad Nacional de Cuyo, R8402AGP Bariloche, Argentina;* orcid.org/0000-0003-1484-061X

Complete contact information is available at: https://pubs.acs.org/10.1021/acs.jpcc.0c03395

Notes

The authors declare no competing financial interest.

ACKNOWLEDGMENTS

We acknowledge the financial support from the following Argentine institutions: CONICET (Grant PIP-2015-00274), ANPCYT (Grant PICT-2015-0922), UNCuyo (Grant 06/C498). We thank the "Centro de Simulación Computacional p/Aplicaciones Tecnológicas" (CSC-CONICET) for granting the use of computational resources which allowed us to perform part of the simulations included in this work.

REFERENCES

(1) Stepanow, S.; Lingenfelder, M.; Dmitriev, A.; et al. Steering molecular organization and host-guest interactions using two-dimensional nanoporous coordination systems. *Nat. Mater.* **2004**, *3*, 229−233.

(2) Gambardella, P.; Stepanow, S.; Dmitriev, A.; et al. Supramolecular control of the magnetic anisotropy in two-dimensional high-spin Fe arrays at a metal interface. *Nat. Mater.* **2009**, *8*, 189−193.

(3) Gutzler, R.; Stepanow, S.; Grumelli, D.; Lingenfelder, M.; Kern, K. Mimicking Enzymatic Active Sites on Surfaces for Energy Conversion Chemistry. *Acc. Chem. Res.* **2015**, *48*, 2132−2139.

(4) Dong, L.; Gao, Z.; Lin, N. Self-assembly of metal-organic coordination structures on surfaces. *Prog. Surf. Sci.* **2016**, *91*, 101−135.

(5) Blowey, P.; Velari, S.; Rochford, L.; Duncan, D.; Warr, D.; Lee, T.-L.; De Vita, A.; Costantini, G.; Woodruff, D. Re-evaluating how charge transfer modifies the conformation of adsorbed molecules. *Nanoscale* **2018**, *10*, 14984−14992.

(6) Tseng, T.-C.; Lin, C.; Shi, X.; Tait, S.; Liu, X.; Starke, U.; Lin, N.; Zhang, R.; Minot, C.; Hove, M. A. V.; et al. Two-dimensional metal-organic coordination networks of Mn-7,7,8,8-tetracyanoquinodimethane assembled on Cu(100): Structural, electronic, and magnetic properties. *Phys. Rev. B: Condens. Matter Mater. Phys.* **2009**, *80*, 155458.

(7) Tseng, T.-C.; Abdurakhmanova, N.; Stepanow, S.; Kern, K. Hierarchical Assembly and Reticulation of Two-Dimensional Mn- and Ni-TCNQ$_x$ (x = 1, 2, 4) Coordination Structures on a Metal Surface. *J. Phys. Chem. C* **2011**, *115*, 10211−10217.
(8) Faraggi, M.; Jiang, N.; Gonzalez-Lakunza, N.; Langner, A.; Stepanow, S.; Kern, K.; Arnau, A. Bonding and charge transfer in metal-organic coordination networks on Au(111) with strong acceptor molecules. *J. Phys. Chem. C* **2012**, *116*, 24558−24565.
(9) Faraggi, M.; Golovach, V.; Stepanow, S.; Tseng, T.-C.; Abdurakhmanova, N.; Kley, C.; Langner, A.; Sessi, V.; Kern, K.; Arnau, A. Modeling Ferro- and Antiferromagnetic Interactions in Metal-Organic Coordination Networks. *J. Phys. Chem. C* **2015**, *119*, 547−555.
(10) Blanco-Rey, M.; Sarasola, A.; Nistor, C.; Persichetti, L.; Stamm, C.; Piamonteze, C.; Gambardella, P.; Stepanow, S.; Otrokov, M.; Golovach, V.; et al. Magnetic Properties of Metal−Organic Coordination Networks Based on 3d Transition Metal Atoms. *Molecules* **2018**, *23*, 964.
(11) Abdurakhmanova, N.; Tseng, T.-C.; Langner, A.; Kley, C.; Sessi, V.; Stepanow, S.; Kern, K. Superexchange-mediated ferromagnetic coupling in two-dimensional Ni-TCNQ networks on metal surfaces. *Phys. Rev. Lett.* **2013**, *110*, 027202.
(12) Ma, Y.; Dai, Y.; Wei, W.; Yu, L.; Huang, B. Novel Two-Dimensional Tetragonal Monolayer: Metal-TCNQ Networks. *J. Phys. Chem. A* **2013**, *117*, 5171−5177.
(13) Deng, Q.; Zhao, J.; Wu, T.; Chen, G.; Hansen, H. A.; Vegge, T. 2D transition metal-TCNQ sheets as bifunctional single-atom catalysts for oxygen reduction and evolution reaction (ORR/OER). *J. Catal.* **2019**, *370*, 378−384.
(14) Pussi, K.; AlShamaileh, E.; McLoughlin, E.; Cafolla, A.; Lindroos, M. Determination of the structure of Cu{100}-p($3\sqrt{2} \times \sqrt{2}$)*R*45°-Sn by dynamical LEED. *Surf. Sci.* **2004**, *549*, 24−30.
(15) Fuhr, J. D.; Gayone, J. E.; Martínez-Blanco, J.; Michel, E. G.; Ascolani, H. Structural and electronic properties of ($3\sqrt{2} \times \sqrt{2}$) *R*45°-Sn/Cu(100): Density functional theory and scanning tunneling microscopy. *Phys. Rev. B: Condens. Matter Mater. Phys.* **2009**, *80*, 115410.
(16) Carrera, A.; Cristina, L.; Bengió, S.; Cossaro, A.; Verdini, A.; Floreano, L.; Fuhr, J.; Gayone, J.; Ascolani, H. Controlling Carboxyl Deprotonation on Cu(001) by Surface Sn Alloying. *J. Phys. Chem. C* **2013**, *117*, 17058−17065.
(17) Fuhr, J.; van der Meijden, M.; Cristina, L.; Rodríguez, L.; Kellogg, R.; Gayone, J.; Ascolani, H.; Lingenfelder, M. Chiral expression of adsorbed (MP) 5-amino[6]helicenes: from random structures to dense racemic crystals by surface alloying. *Chem. Commun.* **2017**, *53*, 130−133.
(18) Quiroga Argañaraz, B.; Cristina, L.; Rodríguez, L.; Cossaro, A.; Verdini, A.; Floreano, L.; Fuhr, J.; Gayone, J.; Ascolani, H. Ubiquitous deprotonation of terephthalic acid in the self-assembled phases on Cu(100). *Phys. Chem. Chem. Phys.* **2018**, *20*, 4329.
(19) Fuhr, J.; Robino, L.; Rodríguez, L. M.; Verdini, A.; Floreano, L.; Ascolani, H.; Gayone, J. 2D Cu-TCNQ Metal-Organic Networks Induced by Surface Alloying. *J. Phys. Chem. C* **2020**, *124*, 416−424.
(20) Wells, J.; Cabailh, G.; Evans, D.; Evans, S.; Bushell, A.; Vearey-Roberts, A. An XPS study of the interaction between tin(II) phthalocyanine and polycrystalline iron. *J. Electron Spectrosc. Relat. Phenom.* **2004**, *141*, 67−72.
(21) Doyle, C. M.; Cunniffe, J. P.; Krasnikov, S. A.; Preobrajenski, A. B.; Li, Z.; Sergeeva, N. N.; Senge, M. O.; Cafolla, A. A. Ni−Cu ion exchange observed for Ni(II)−porphyrins on Cu(111). *Chem. Commun.* **2014**, *50*, 3447.
(22) Shen, K.; Narsu, B.; Ji, G.; Sun, H.; Hu, J.; Liang, Z.; Gao, X.; Li, H.; Li, Z.; Song, B.; et al. On-surface manipulation of atom substitution between cobalt phthalocyanine and the Cu(111) substrate. *RSC Adv.* **2017**, *7*, 13827.
(23) Williams, C. G.; Wang, M.; Skomski, D.; Tempas, C. D.; Kesmodel, L. L.; Tait, S. L. Metal-Ligand Complexation through Redox Assembly at Surfaces Characterized by Vibrational Spectroscopy. *J. Phys. Chem. C* **2017**, *121*, 13183−13190.
(24) Blowey, P.; Sohail, B.; Rochford, L.; Lafosse, T.; Duncan, D. A.; Ryan, P. T. P.; Warr, D. A.; Lee, T.-L.; Costantini, G.; Maurer, R. J.; et al. Alkali Doping Leads to Charge-Transfer Salt Formation in a Two-Dimensional Metal-Organic Framework. *ACS Nano* **2020**, *14*, 7475−7483.
(25) Hötger, D.; Abufager, P.; Morchutt, C.; Alexa, P.; Grumelli, D.; Dreiser, J.; Stepanow, S.; Gambardella, P.; Busnengo, H.; Etzkorn, M.; et al. On-surface transmetalation of metalloporphyrins. *Nanoscale* **2018**, *10*, 21116−21122.
(26) Gotter, R.; Ruocco, A.; Morgante, A.; Cvetko, D.; Floreano, L.; Tommasini, F.; Stefani, G. The ALOISA end station at Elettra:: a novel multicoincidence spectrometer for angle resolved APECS. *Nucl. Instrum. Methods Phys. Res., Sect. A* **2001**, *467*, 1468−1472.
(27) Floreano, L.; Naletto, G.; Cvetko, D.; Gotter, R.; Malvezzi, M.; Marassi, L.; Morgante, A.; Santaniello, A.; Verdini, A.; Tommasini, F.; et al. Performance of the grating-crystal monochromator of the ALOISA beamline at the Elettra Synchrotron. *Rev. Sci. Instrum.* **1999**, *70*, 3855−3865.
(28) Giannozzi, P.; Baroni, S.; Bonini, N.; Calandra, M.; Car, R.; Cavazzoni, C.; Ceresoli, D.; Chiarotti, G. L.; Cococcioni, M.; Dabo, I.; et al. QUANTUM ESPRESSO: a modular and open-source software project for quantum simulations of materials. *J. Phys.: Condens. Matter* **2009**, *21*, 395502.
(29) Hamada, I. van der Waals density functional made accurate. *Phys. Rev. B: Condens. Matter Mater. Phys.* **2014**, *89*, 121103.
(30) Lee, K.; Murray, E. D.; Kong, L.; Lundqvist, B. I.; Langreth, D. C. Higher-accuracy van der Waals density functional. *Phys. Rev. B: Condens. Matter Mater. Phys.* **2010**, *82*, 081101.
(31) Cococcioni, M.; de Gironcoli, S. Linear response approach to the calculation of the effective interaction parameters in the LDA + U method. *Phys. Rev. B: Condens. Matter Mater. Phys.* **2005**, *71*, 035105.
(32) Jónsson, H.; Mills, G.; Jacobsen, K. W. Nudged elastic band method for finding minimum energy paths of transitions. In *Classical and Quantum Dynamics in Condensed Phase Simulations*; World Scientific, 1998; pp 385−404.
(33) In a previous work,[34] we have determined that 125 °C is the maximum temperature at which the Sn-TCNQ network synthesized on Au(111) is stable. The fact that the Cu−nitrile interaction is considerably stronger than the Sn−nitrile interaction[19] indicates that the thermal stability of the β and γ phases should be above that temperature.
(34) Rodríguez, L. M.; Fuhr, a J. D.; Machaín, P.; Ascolani, H.; Lingenfelder, M.; Gayone, J. E. Building two-dimensional metal−organic networks with tin. *Chem. Commun.* **2019**, *55*, 345−348.
(35) Mabrouk, M.; Hayn, R. Magnetic moment formation in metal-organic monolayers. *Phys. Rev. B: Condens. Matter Mater. Phys.* **2015**, *92*, 184424.
(36) Tersoff, J.; Hamann, D. R. Theory of the scanning tunneling microscope. *Phys. Rev. B: Condens. Matter Mater. Phys.* **1985**, *31*, 805−813.
(37) van der Marel, D.; Westra, C.; Sawatzky, G. A.; Hillebrecht, F. U. Electronic structure of Mn impurities in noble metals. *Phys. Rev. B: Condens. Matter Mater. Phys.* **1985**, *31*, 1936.
(38) Kimura, A.; Asanao, S.; Kambe, T.; Xie, T.; Watanabe, S.; Taniguchi, M.; Qiao, S.; Hashimoto, E.; Namatame, H.; Muro, T.; et al. Electron correlation and magnetic properties of c(2 × 2)CuMn/Cu(001) two-dimensional surface alloys. *Phys. Rev. B: Condens. Matter Mater. Phys.* **2007**, *76*, 115416.
(39) Krüger, P.; Kotani, A. Calculation of core-level photoemission spectra of Mn films on Ag(001). *Phys. Rev. B: Condens. Matter Mater. Phys.* **2003**, *68*, 035407.
(40) Gayone, J. E.; Carrera, A.; Grizzi, O.; Bengió, S.; Sánchez, E. A.; Martínez-Blanco, J.; Michel, E. G.; Fuhr, J. D.; Ascolani, H. Order-disorder phase transition of vacancies in surfaces: The case of Sn/Cu(001)-0.5 ML. *Phys. Rev. B: Condens. Matter Mater. Phys.* **2010**, *82*, 035420.
(41) Shi, Z.; Liu, J.; Lin, T.; Xia, F.; Liu, P. N.; Lin, N. Thermodynamics and Selectivity of Two-Dimensional Metallo-

https://dx.doi.org/10.1021/acs.jpcc.0c03395
J. Phys. Chem. C XXXX, XXX, XXX−XXX

supramolecular Self-Assembly Resolved at Molecular Scale. *J. Am. Chem. Soc.* **2011**, *133*, 6150−6153.
(42) Chen, Y.; Liu, J.; Sun, Q.; Kawazoe, Y.; Jena, P. Bipolar Magnetic Materials Based on 2D Ni[TCNE] Metal-Organic Coordination Networks. *Adv. Electron. Mater.* **2018**, *4*, 1700323.

https://dx.doi.org/10.1021/acs.jpcc.0c03395
J. Phys. Chem. C XXXX, XXX, XXX−XXX